Chiroptical Properties of Chiral Substituted Polyfluorenes

M. Oda,[†,#] H.-G. Nothofer,[‡,+] U. Scherf,[*,‡] V. Šunjić,[§] D. Richter,[⊥] W. Regenstein,[†] and D. Neher[*,†]

Universität Potsdam, Institut für Physik, Am Neuen Palais 10, D-14469 Potsdam, Germany; Universität Potsdam, Institut für Chemie, Karl-Liebknechtstr. 24-25, Haus 25, D-14476 Golm, Germany; Rudjer Boskovic Inststitute, Lab. of Stereoselective Catalysis & Biocatalysis, POB 180, Bijenicka Cesta 54, HR-10002 Zagreb, Croatia; and Max-Planck-Institut für Polymerforschung, Ackermannweg 10, D-55128 Mainz, Germany

Received April 22, 2002; Revised Manuscript Received June 25, 2002

ABSTRACT: Liquid-crystalline polyfluorene (PF) homopolymers substituted with chiral alkyl side chains were synthesized, and their chiroptical properties in the solid state were investigated by means of circular dichroism (CD), circularly polarized photoluminescence (CPPL), and circularly polarized electroluminescence (CPEL) measurements. Polarization-selective scattering of light is shown to cause artifacts in the circularly polarized absorption and emission spectra in the wavelength range near or above the absorption edge, and a measurement scheme to avoid these is presented. For all derivatives, significant chiroptical effects appeared only after the solid layers have been annealed at elevated temperatures, preferably into the liquid-crystalline state of the polymer. The largest anisotropy factors were measured for a polyfluorene substituted with chiral (*R*)-2-ethylhexyl side chains, yielding absolute values of up to 0.28 for CPPL and up to 0.25 for CPEL. These are among the highest ever reported for a chiral conjugated polymer. Anisotropy factors for CD, CPEL, and CPPL were consistently found to follow an "odd−even effect" concerning the position of the chiral center in the alkyl side chain. If the chiral center is placed close to the polymer backbone, the CD is dominated by one peak with its maximum close to the maximum of the $\pi-\pi^*$ absorption band. This indicates that the chiroptical properties are most probably caused by *intra*chain effects rather than by pure *inter*chain exciton coupling. This interpretation is supported by the results of time-dependent Hartree−Fock calculations for the isolated fluorene dimer and trimer. In both cases, the anisotropy factor depends strongly on the torsion angle between neighboring fluorene units. For the trimer, a maximum anisotropy factor of 0.25, close to the maximum values determined experimentally, is predicted for a torsion angle of ca. 105°. Both experimental and theoretical results indicate that the chiroptical properties of these chiral substituted polyfluorenes are mainly caused by a helical conformation of the conjugated polymer backbone.

Introduction

Substituted polyfluorenes are promising materials for polymer light-emitting diodes (PLED), especially because of their blue and strong electroluminescence and their good solubility in organic solvents, which is necessary for the preparation of homogeneous layers with solution-based coating techniques.[1−3] With proper choice of the side chains, these polymer exhibit liquid crystalline (LC) phases, which allows for the orientation of the polymer in thin solid films on suitable alignment layers.[4−7] Those aligned polyfluorene layers have recently been utilized in devices with highly polarized electroluminescence.[8−10]

In 2000, we demonstrated that chiral substituted polyfluorenes film exhibit extraordinary chiroptical properties.[11,12] In particular, we have been able to prepare devices with circularly polarized electroluminescence (CPEL). Light sources with large degrees of CPEL are of interest as backlights for liquid crystal display.[13] For poly(9,9-bis((3*S*)-3,7-dimethyloctyl)fluorene-2,7-diyl) (PF8/1/1) and poly(9,9-bis((*S*)-2-methylbutyl)fluorene-2,7-diyl) (PF4/1), the anisotropy factors g, defined as $g = 2(I_L - I_R)/(I_L + I_R)$ (where I_L and I_R are the left- and right-handed emission intensities, respectively), have been found to be up to 0.25. This is much larger than the value of $g_{CPEL} = 0.0013$ reported by Meijer et al. in 1997 for the first circularly polarized LED, which utilized a chiral substituted PPV derivative.[14] Up to now, these are the only reports on CPEL generated by an organic optically active emission layer.

In this paper we report our further investigation of chiral polyfluorenes. Especially, we present the chiroptical properties of poly(9,9-bis((*R*)-2-ethylhexyl)fluorene-2,7-diyl), the chiral analogue of the often used racemic poly(9,9-bis(2-ethylhexyl)fluorene-2,7-diyl) (PF2/6). CD and circularly polarized photoluminescence (CPPL) spectra of polyfluorenes with different chiral alkyl side chains are discussed with respect to *intra*- and *inter*chain contributions to the chiroptical response. These interpretations are supported by Hartree−Fock calculations of the anisotropy factor of fluorene oligomers.

Experimental and Calculation Method

Chiral substituted polyfluorenes (Figure 1), poly(9,9-bis((*S*)-2-methylbutyl)fluorene-2,7-diyl) ((S)-PF4/1), poly(9,9-di-*n*-octyl-*co*-9,9-bis((*S*)-2-methylbutyl)fluorene-2,7-diyl) ((S)-PF4/1-*co*-PF8), poly(9,9-bis((3*S*)-3,7-dimethyloctyl)fluorene-2,7-diyl) ((S)-PF8/1/1), poly(9,9-bis((*S*)-5-methylheptyl)fluorene-2,7-diyl) ((S)-PF7/1), and poly(9,9-bis((*R*)-2-ethylhexyl)fluorene-2,7-diyl) ((R)-PF2/6), were synthesized via Yamamoto-type polycondensation

[†] Universität Potsdam, Institut für Physik.
[‡] Universität Potsdam, Institut für Chemie.
[§] Rudjer Boskovic Inststitute.
[⊥] Max-Planck-Institut für Polymerforschung.
[#] Present address: Sony Corporation, Fusion Domain Laboratory, R&D Group, Haneda Tec. 5-21-15 Higashikojiya Ota-ku, 144-0033 Tokyo, Japan.
[+] Present address: SONY International (Europe) Gmbh, Stuttgart Technology Center, Stuttgarter Strasse 106, D-70736 Fellbach, Germany.
* To whom correspondence should be addressed. E-mail neher@rz.uni-potsdam.de or scherf@rz.uni-potsdam.de.

10.1021/ma020630g CCC: $22.00
Published on Web 07/24/2002

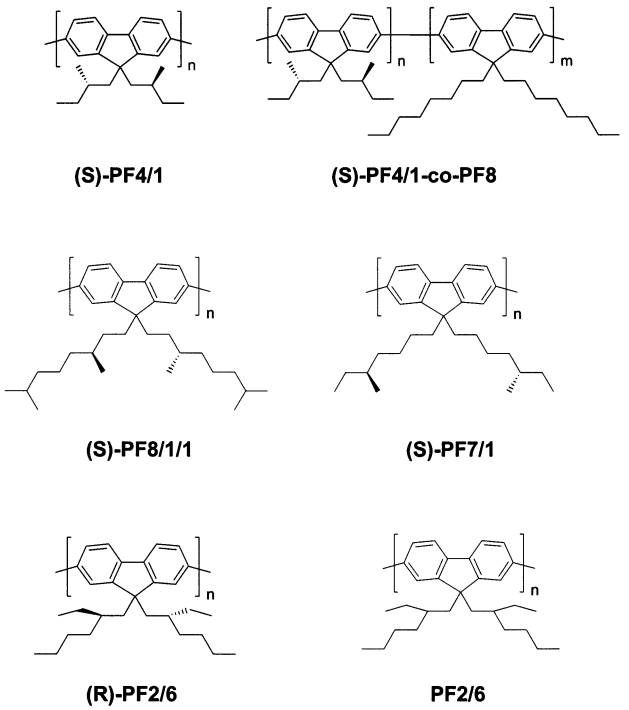

Figure 1. Polyfluorenes with chiral side chains.

Table 1. Molecular Weights (GPC/PS Calibration) and LC Phase Transition Temperatures T_{LC} of Chiral Substituted Polyfluorenes

	M_n	M_w	T_{LC} (°C)
(S)-PF4/1	30 000	56 000	>250
(S)-PF4/1-*co*-PF8	125 000	282 000	190
(S)-PF8/1/1	170 000	290 000	105
(R)-PF2/6	85 500	184 000	165
(S)-PF7/1	203 000	405 500	230

with $Ni(COD)_2$ as an effective aryl−aryl coupling agent. Biocatalytically[15] obtained (*R*)-2-ethylhexanol (99% e.e.) was used for the synthesis of (R)-PF2/6. Achiral, racemic poly(9,9-bis(2-ethylhexyl)fluorene-2,7-diyl) (PF2/6) was also investigated as a reference. Molecular weights as well as phase transition temperatures of these polymers are summarized in Table 1. A crystal to liquid crystal (C−LC) phase transition was observed for (S)-PF4/1-*co*-PF8, (S)-PF8/1/1, (S)-PF7/1, (R)-PF2/6, and PF2/6. More details of the synthesis and characterization are given in ref 16.

For optical experiments, PFs were spin-coated onto fused silica substrates from toluene solution. Then, the samples were annealed in a vacuum oven up to 200 °C for 5−10 h. Light-emitting diodes were prepared on indium−tin oxide (ITO) substrates. A thermally evaporated Al electrode served as the cathode. All optical measurements were carried out at room temperatures in ambient conditions.

UV/vis absorption spectra were measured with a Perkin-Elmer Lambda 19 spectrometer. Circular dichroism (CD) spectra were measured with a JASCO 710 or a JASCO 700 spectrometer. Photoluminescence (PL) spectra were measured with a Photon Technology International Inc. alpha-scan type spectrometer equipped with single path monochromators to select the wavelength of excitation and emission and with a single photon counting detection.

Circularly polarized photoluminescence (CPPL) and electroluminescence (CPEL) spectra were measured with the PTI photospectrometer in combination with a differential photon counting (DPC) system, based on the principal design described in ref 17. A photoelastic modulator (PEM) of Hinds Co. acts as a time-variable wave plate. When set to quarter-wave retardation, the modulator will periodically convert circularly polarized light into linear-polarized light, while nonpolarized light is not affected at all. The CP component in the emitted light is then detected by placing a linear sheet polarizer behind the PEM in combination with gated single-photon detection. For CPPL measurement, the polymer layer sample was excited through the substrate, perpendicular to the substrate surface, via an optical fiber and a lens. The final spot size on the sample was ca. 1 mm in diameter. An interference filter with maximum transmission at the selected excitation wavelength was inserted between the fiber and the sample to suppress stray light passing the single monochromator of the excitation path. The emission was detected from the front side perpendicular to the sample surface. A pinhole (1 mm diameter) was placed directly behind the sample in order to avoid scattering effects as discussed below.

Table 2. Maximum Anisotropy Factors *g* of Chiral Substituted Polyfluorenes in Circular Dichroism (g_{CD}), Circularly Polarized Photoluminescence (g_{CPPL}), and Circularly Polarized Electroluminescence (g_{CPEL})

	g_{CD}	g_{CPPL}	g_{CPEL}
(S)-PF4/1	>0.15[a]		0.16[b]
(S)-PF4/1-*co*-PF8	0.04		0.05[b]
(S)-PF8/1/1	<−0.15[a]	−0.25	−0.25[b]
(R)-PF2/6	<−0.15[a]	−0.28	−0.25
(S)-PF7/1	−0.004		

[a] In the case of (S)-PF4/1, (S)-PF8/1/1, and (R)-PF2/6, the maximum g_{CD} could not accurately be determined since the response exceeded the measurement range of our CD spectrometer. [b] From ref 3.

Ab initio molecular orbital (MO) calculations were carried out using the Gaussian 98 program on a DEC 2100 4/266 workstation and the Gaussian 98W program on a PC with Pentium 4 processor. Partial structural optimizations of the fluorene dimer and trimer for each torsion angle between neighboring monomers were carried out by the RHF method with 6-31G (d) (d type diffuse function on C) basis set. The torsion angle dependent S_0-S_1 transition energy as well as electric transition dipole moment and magnetic transition dipole moment of fluorene dimer and trimer were calculated by the time-dependent (TD) Hartree−Fock method within the Gaussian 98 program with the 6-31G (d) basis set.

Results

Circular Polarization in Absorption and Emission. UV−vis absorption and CD spectra of the (*R*)-PF2/6 thin film are shown in parts a and b of Figure 2, respectively, in comparison with those of (*S*)-PF8/1/1, (*S*)-PF4/1, and (S)-PF7/1 thin layers. The maximum *g* values in CD of all PF derivatives are summarized in Table 2, together with the values determined in CPPL and CPEL. The solid-state absorption maxima are significantly different; (R)-PF2/6 and (S)-PF4/1 show broad, unstructured absorption bands peaking at 385 and 368 nm, respectively. The UV−vis spectra of (S)-PF8/1/1 and (S)-PF7/1 display additional lower energy features at 394 and 397 nm, respectively. These lower energy peaks (shoulders) indicate the formation of chains with improved *intrachain* order.[18] All chiral PF derivatives show some tailing of the absorption spectra near the absorption edges, caused by light scattering effects of the liquid crystalline, anisotropic polymer films, most pronounced for (R)-PF2/6 and (S)-PF7/1.

For PF7/1, in which the asymmetric carbon center possesses a larger distance from the polyfluorene backbone in relation to all other chiral PF derivatives, the chiroptical response is only weak. In this case, the CD exhibits a weak, bisignate Cotton effect, indicative of *inter*chain exciton coupling as the origin for the observed effect. The positive and negative lobes peak at 351 and 398 nm, respectively, with a zero point at 374 nm.

All other chiral derivatives display asymmetric, bisignate CD peaks of much higher intensity. While the CD

of PF4/1 still exhibits a rather bisignate shape, the CD of (R)-PF2/6 and (S)-PF8/1/1 is dominated by one peak with its maximum close to the maximum of the $\pi-\pi^*$ absorption band. These dominating signals are accompanied by weaker higher energy lobes ((R)-PF2/6: 342 nm, zero point at 357 nm and (S)-PF8/1/1). The shape of the CD bands indicates that other (most probably *intra*chain) effects cover the contribution from a pure *inter*chain exciton coupling, the CD spectra thus resulting from *inter*chromophore interactions as well as a chiral (helical) *intra*chromophore conformation.[19,20] The CD spectra of (R)-PF2/6 and (S)-PF8/1/1 display additional low-energy bands peaking around 420 nm which are located in the tail of the absorption bands. Especially in the case of (R)-PF2/6 thin films, this CD peak at around 420 nm was found to be relatively strong. This band is absent in the spectrum of (S)-PF4/1, even though this compound also exhibits strong chiroptical effects. Please note that the annealing of the films at 200 °C is distinctly above the LC phase transition temperature for (R)-PF2/6 and (S)-PF8/1/1, while (S)-PF4/1 softens at much higher temperature (>250 °C). In fact, layers of the two former compounds looked quite milky after annealing and polarized microscopy revealed typical nematic Schlieren textures. Therefore, we conclude that the low-energy CD band is not due to the inherent properties of the chiral polymers. The appearance of the low-energy CD band of (R)-PF2/6 and (S)-PF8/1/1 rather indicates the existence of non-absorption-related CD effects in the wavelength region >410 nm caused by light scattering of the liquid crystalline, anisotropic polymer films.

The film absorption spectra differ slightly from those measured in solution (Figure 2c). For PF2/6 and PF8/1/1, the film spectra noticeably broaden toward longer wavelengths compared to the solution spectra. While part of the effect might be due to scattering as discussed below, it might also indicate an improved intrachain or interchain order after annealing in the solid state, induced by the particular side chain architecture. For PF4/1 both the solution and the film absorption spectra are blue-shifted compared to the spectra of all other derivatives studied here. Note that PF4/1 shows the lowest number-average molecular weight (GPC, PS calibration: 29.000) among the chiral PF derivatives due to the only moderate solubilizing power of the methylbutyl side groups. This lower M_n value might explain in part the observed blue shift in solution and in the solid state.

Circular Polarization in Emission. The overall photoluminescence (PL) spectrum (excitation at 365 nm) and the spectral dependence of the anisotropy factor g_{CPPL} of the circularly polarized PL for a thin (R)-PF2/6 film are depicted in parts a and b of Figure 3, respectively. Since artifacts in circularly polarized emission spectroscopy arise whenever the emission is linearly polarized,[21] the degree of linear polarization was carefully checked in each case, and only samples that yielded negligible linear contributions were studied further. The PL spectrum displays peaks at 422 nm (maximum) and 439 nm (shoulder). A strong CPPL signal was observed which peaks at ca. 430 (negative lobe) and 405 nm (positive lobe) whereby the lower energy contribution dominates the CPPL spectrum. The anisotropy factor g_{CPPL} of the circularly polarized photoluminescence at 430 nm depends on the conditions of film preparation, its absolute value varies from 0.12 to 0.28. The intensity

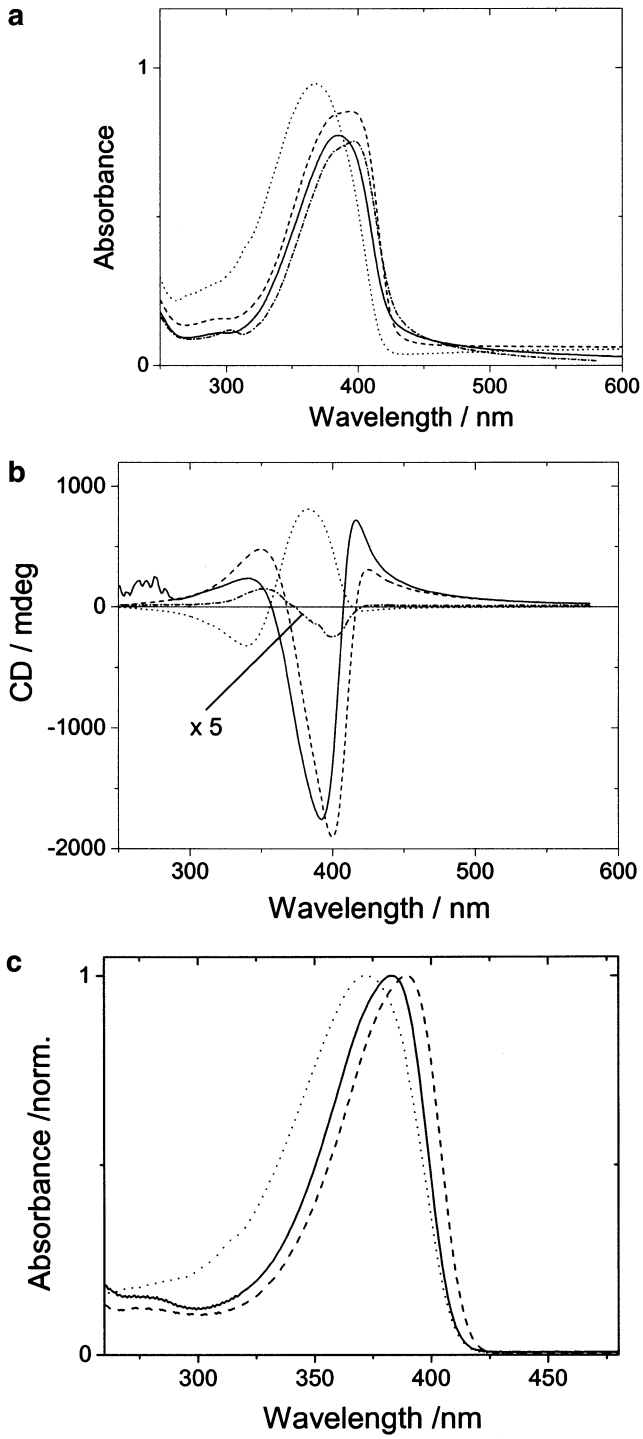

Figure 2. (a) UV−vis spectra of chiral (R)-PF2/6 (solid line), (S)-PF8/1/1 (dash line), (S)-PF4/1 (dot line), and (S)-PF7/1 (dash−dot line) thin films (ca. 60 nm) on fused silica substrates, annealed for 5 h/200 °C under argon. (b) CD spectra of chiral (R)-PF2/6 (solid line), (S)-PF8/1/1 (dash line), (S)-PF4/1 (dot line), and (S)-PF7/1 (dash−dot line) thin films (ca. 60 nm) on fused silica substrates, annealed for 5 h/200 °C under argon, all films display linear dichroisms of <0.01%. (c) Normalized absorption spectra of (R)-PF2/6 (solid line), (S)-PF8/1/1 (dash line), and (S)-PF4/1 (dot line) in dilute chloroform solution (ca. 10^{-5} mol/L).

of the peak at 405 nm is strongly influenced by the location of the excitation spot with respect to the pinhole placed behind the sample (as shown in Figure 3b). If the excitation spot is slightly deadjusted with respect to the pinhole, the peak at around 405 nm distinctly

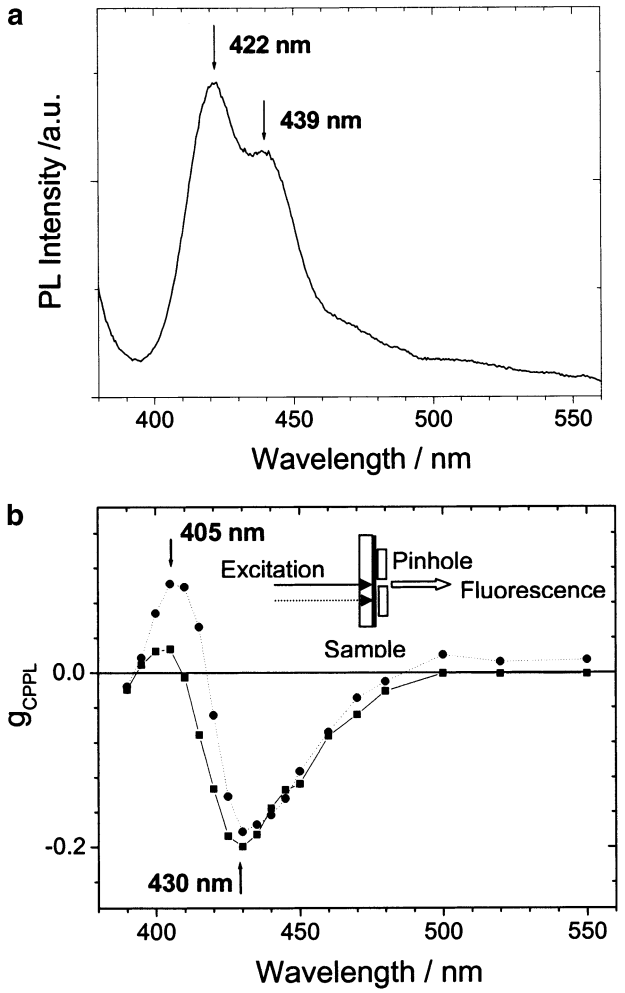

Figure 3. Total (a) and circularly polarized (b) photoluminescence intensity of a 60 nm thick film of (R)-PF2/6. The excitation wavelength was 365 nm. Circularly polarized photoluminescence (CPPL) was measured using the sample holder with a pinhole. The excitation spot was either placed directly at the position of the pinhole (solid line, squares) or slightly displaced from this position (dashed line, circles). In the latter case, part of the emitted light can reach the detector only when scattered within the layer.

increases while the signal at 430 nm merely changes. Therefore, we assign this peak to stem from light scattering effects. Most likely, light generated by PL is scattered within the layer by the liquid-crystalline domains before being emitted through the pinhole. If we presume that the efficiency of scattering is different for right- and left-handed polarized light, the signal finally detected by the setup should have a circularly polarized component, even if the light originally emitted by the polymer layer is not polarized.

Further proof that the peak is caused by scattering effects comes from the comparison of the CD signal and the CPPL spectrum. In the CPPL spectrum shown in Figure 3b the scattering peak has a positive g value, indicating that left-handed light is scattered more efficiently. In the CD experiment, the absorption of light is measured in transmission, and therefore, any scattering creates an (artificial) absorption contribution. In fact, the long wavelength CD peak has a positive sign, indicating that left-handed light is scattered more efficiently, in agreement with the CPPL data. If, however, the pinhole is placed directly at the excitation spot, the emission signal is dominated by photons leaving the sample without further being scattered in the layer, and the peak at 405 nm is strongly suppressed.

For circularly polarized electroluminescence CPEL of (R)-PF2/6, the value of the anisotropy factor g_{CPEL} is up to 0.253 at 425 nm (not shown here). The coincidence of the sign and peak position (±5 nm) of CPPL and CPEL indicates that both originate from the same emissive species. The observed values for g_{CPPL} and g_{CPEL} for thin films of (R)-PF2/6 are slightly but significantly increased in comparison to (S)-PF8/1/1.[12] This may be a result of a somewhat higher order of packing due to the shorter side chains of (R)-PF2/6.

Time-Dependent Hartree−Fock Calculation. Hartree−Fock calculations have been carried out to estimate the range of values of the anisotropy factor achievable through *intra*chain effects. The anisotropy factor g is related to the rotational strength R and the dipole strength D by the relation[22]

$$g = \frac{4R}{D} \tag{1}$$

Here, R and D are functions of the electric transition dipole moment $\vec{\mu}$ and magnetic transition dipole moment $\vec{m}$:

$$R = \mathrm{Im}\{\vec{\mu}\cdot\vec{m}\}$$
$$D = |\vec{\mu}|^2 + |\vec{m}|^2 \tag{2}$$

The values and directions of the electric and magnetic transition moments were determined for the S_0-S_1 electronic transition of the fluorene dimer and trimer, utilizing time-dependent Hartree−Fock calculations. The g values calculated from these transition moments are shown in Figure 4 as a function of the torsion angle between the monomer units. For both molecules, the anisotropy factor depends strongly on the torsion angle. In both cases, g is zero for a torsion angle of 0° and 180°, as the corresponding molecular structures do not possess a chiral conformation. For the fluorene dimer, the anisotropy factor as a function of torsion angle has a bisignate shape, with its maximum absolute value of about 0.18 at a torsion angle of ca. 120°. For the fluorene trimer, the value of g is always negative with the maximum absolute value of about 0.25 at a torsion angle of ca. 105°. In recent X-ray and electron diffraction experiments on aligned layers of racemic PF2/6, the conformation of the backbone was determined to be helical, with the helical pitch corresponding to five monomer units. Thus, either a 5_1 helix (torsion angle of about 72°) or a 5_2 helix (torsion angle of about 144°) is a possible conformation. For both torsion angles, the calculations yield values of the anisotropy factor which are well comparable to the measured values for g_{CD}, g_{CPPL}, and g_{CPEL} of chiral substituted polyfluorenes. This indicates that even an isolated helical polyfluorene chain with a proper torsion angle between subsequent monomer units can yield considerably large anisotropy factors. This further suggests that the large values of g in absorption and emission are mainly caused by *intrachain* electronic effects and not by exciton coupling.

Figure 4b,c shows calculated absolute values of the electric transition dipole moment $\mu = |\vec{\mu}|$ and magnetic transition dipole moment $m = |\vec{m}|$ as well as the angle θ between $\vec{\mu}$ and $\vec{m}$. While the value of the electric dipole moment varies only slightly with the torsion angle, both $|\vec{m}|$ and θ exhibit a characteristic dependence. The

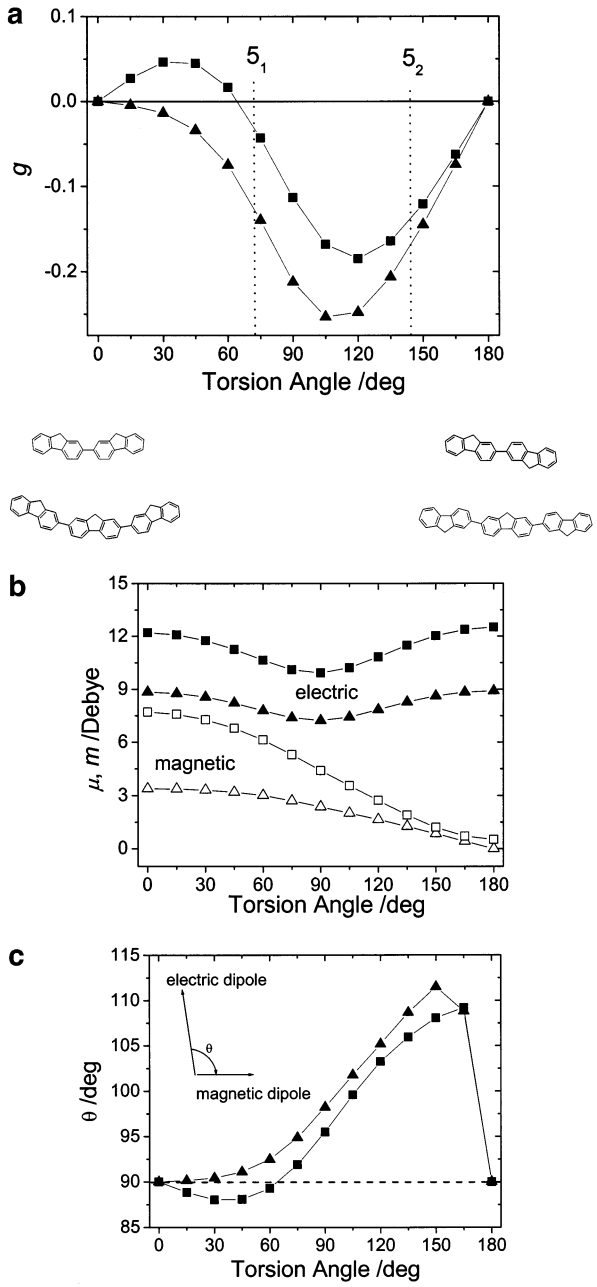

Figure 4. Time-dependent Hartree−Fock (TD-HF) calculation of fluorene oligomers (dimer and trimer), based on RHF/6-31G (d) calculations. (a) Calculated anisotropy factor g of the $S_0 \rightarrow S_1$ transition for the fluorene dimer (squares) and trimer (triangles) as a function of the torsion angle between adjacent monomer units. (b) Absolute values of the electric (solid symbols) and magnetic (open symbols) transition dipole moments of the fluorene dimer (squares) and trimer (circles) as a function of the torsion angle. (c) Angle θ between the electric and the magnetic transition dipole moment vector as a function of the aryl−aryl torsion angle in the fluorene dimer (squares) and trimer (triangles).

absolute value of the magnetic moment decreases monotonically with increasing torsion angle, as the conformation of the oligomers turns from a planar bow with the magnetic dipole directed perpendicular to the plane of the bow into a planar straight chain (which in the ideal case has no magnetic dipole) for a torsion angle of 180°. In between, the structure of the oligomer can be regarded as part of a coil, which possesses a nonzero component of the magnetic dipole parallel to the coil direction. Consequently, the angle θ deviates from 90° when the torsion angle is larger than zero and sharply drops back to 90° when the linear planar chain is attained at a torsion angle of 180°. Thus, the maximum in g at intermediate torsion angles can be understood by the tradeoff between a decrease in the absolute value of the magnetic dipole moment and the increase of θ between the electric and magnetic transition dipole moment with increasing torsion angle.

Table 3. Odd−Even Effect of the Chiroptical Properties of Chiral Substituted Polyfluorenes[a]

position n of chiral carbon center in the alkyl side chain (distance from 9-position of the fluorene unit in no. of carbons)	sign of the anisotropy factor g (PF sample investigated)	
	R	S
2 ($2n$)	− (R)-PF2/6 (*2*)	+ (S)-PF4/1 (*2*)
3 or **5** ($2n + 1$)	+ (no example)	− (S)-PF8/1/1 (*3*), (S)-PF7/1 (*5*)

[a] The sign of the anisotropy factor g refers to that of the most prominent long-wavelength peak in the CD spectrum.

Discussions and Conclusions

If scattering effects as discussed above are ignored, the sign of the dominant peak in the CD spectrum is the same as in the CPPL measurement for each individual chiral polymer. Also, for all polymers except PF7/1, the spectral position of the dominant feature in the CD spectra agrees with the maximum of the main absorption peak in the absorption spectra, which is attributed to the S_0-S_1 transition. In emission, the CPPL signal covers the spectral range of the nonpolarized emission, which has been attributed to the intrachain S_1-S_0 transition of the singlet exciton.[18] This rationalizes the conclusion that the dominant signals in CD and CPPL are due to the lowest $\pi-\pi^*$ singlet transition.

For (R)-PF2/6, (S)-PF4/1, and (S)-PF8/1/1 the size of the anisotropy factor is well above what has been measured for other chiral-substituted conjugated polymers and which had been attributed to *inter*chain exciton coupling.[23] On the basis of the calculations of the anisotropy factor for PF oligomers presented above, it is plausible to suggest that the chiroptical properties are clearly dominated by *intra*chain effects, presuming that the PF backbone adopt a regular helical conformation.

The signs of the dominant chiroptical properties in absorption and emission reflect a so-called odd−even-effect (see Table 3) as proposed by Meijer et al. for chiral polythiophenes.[24,25] (R)-PF2/6 and (S)-PF4/1 with their asymmetric carbons in the 2-position of the alkyl side chain display a negative—(R)-PF2/6—or positive—(S)-PF4/1—bisignate Cotton effect, while (S)-PF8/1/1 with a 3-position of the chiral center displays a positive low-energy lobe. The reason for this correlation between the position of the chiral carbon center and the sign of the anisotropy factor of polyfluorenes is yet not fully understood, but it clearly indicates that the chiroptical effects are due to a side chain induced main chain chirality.[26] On the basis of the strong tendency of racematic PF2/6 to adopt a helical conformation, we had previously presumed that the chiral side chain substituents favor the formation of helices of one energetically preferred helical sense during annealing. As significant anisotropy factors are observed even when the samples

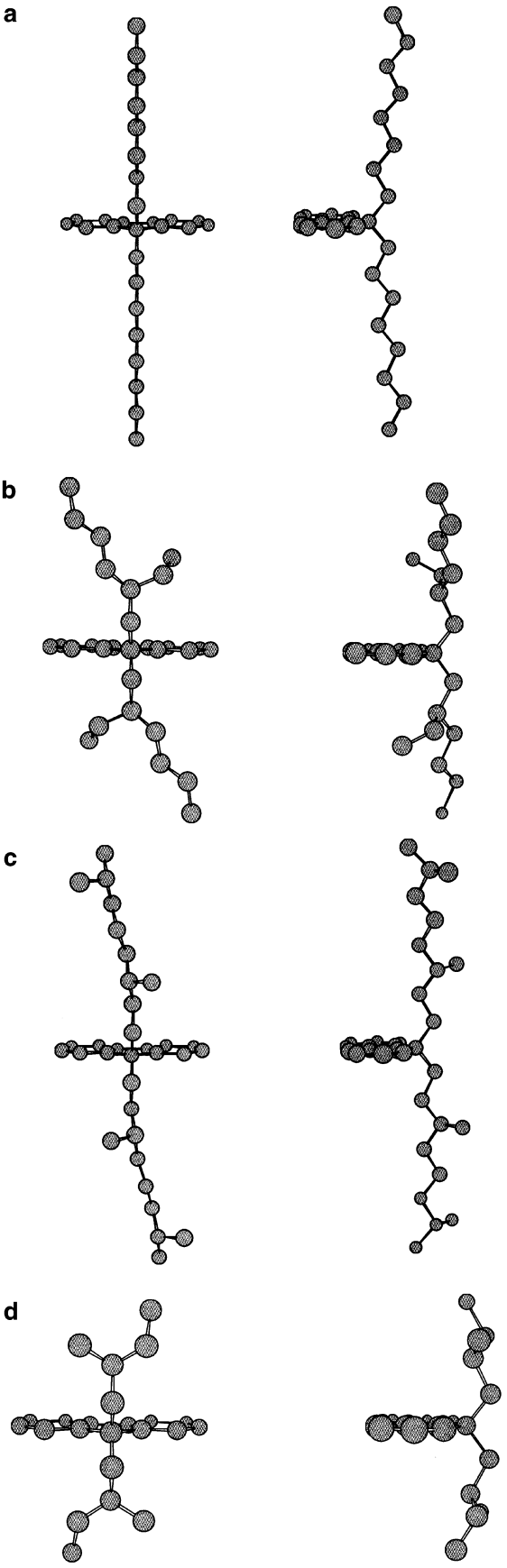

Figure 5. Optimized structures of the monomeric building blocks of (a) PF8, (b) (R)-PF2/6, (c) (S)-PF8/1/1, and (d) (S)-PF4/1, based on RHF/6-31 G calculations. Normal-coordinate analysis were carried out for each optimized structure to prove these structures to be in the energy minimum.

are annealed well below the transition to the LC phase (e.g., for PF4/1), we presume that the formation of a regular helix does not require the motion of the PF chains as a whole but occurs via local changes of the torsion angles between adjacent monomer units. Recent simulations on PF dimers have shown that the energy barrier for the reversal of the torsion angle (e.g., from 45° to 135°) is in the range of only 2 eV, and the pronounced thermochromic effects in PF layers have been attributed to this low barrier.[27,28] It can, therefore, be concluded that a nonhelical backbone characterized by a statistical variation of torsion angles can be converted into a regular helix with a narrow distribution of torsion angles without the requirement of large-scale motion of longer segments of the polymer backbone.

To get further inside into the parameters controlling the sign of the chiroptical response, we have performed simulations on the conformation of the side chains. Figure 5 shows the optimized structures of the monomeric building blocks of (a) PF8, (b) (R)-PF2/6, (c) (S)-PF8/1/1, and (d) (S)-PF4/1. In the case of PF8 (Figure 5a) the conformation of the octyl side chain is zigzag, with the alkyl chains perpendicular to the plane of the fluorene group. This result of our simulation is in agreement with X-ray investigations on well-ordered samples of PF8.[18] Note, however, that the PF backbone in these well-ordered samples adopt a planar conformation,[18,29] which gives rise to a new absorption feature at 436 nm. This spectral feature is not observed in any of the nonannealed or annealed layers of the polymers presented here. In contrast to the octyl chain in PF8, the branched alkyl side chains of PF2/6, PF8/1/1, and PF4/1 are not completely perpendicular to the fluorene plane, as shown in the left side of Figure 5b−d. In a view of the monomeric unit from the 9,9-position, the hexyl chain of the (R)-PF2/6 (Figure 5b) and the octyl chain of the (S)-PF8/1/1 building blocks (Figure 5c) are directed from upper-left to lower-right. On the other hand, the butyl chain of the (S)-PF4/1 building block extends from the upper-right to lower-left direction. As the anisotropy factor in absorption and emission of the thin film of (R)-PF2/6 and (S)-PF8/1/1 is negative while that (S)-PF4/1 is positive, we presume that the direction of the longest segment of the branched side chains determines the sign of the anisotropy factor. However, note the force field simulations of isolated monomeric units will only give a very rough imagination of the real solid-state packing of the PF polymer chains.

Finally, we note that other approaches have been demonstrated to realize large *g* values in absorption and emission based on conjugated polymers. As an example, Grell et al. reported a circularly polarized light-emitting diode utilizing a chiroselective reflector.[30] This device emitted green light with an anisotropy factor of up to 1.6. However, this diode used an emission layer based on an achiral polyfluorene derivative, and the chiroptical emission properties of this device were not related to the electronic structure of the emitter. Very recently, solid layers of chiral substituted poly(*p*-phenylene ethynylene) copolymers exhibited absolute *g* values in CD of up to 0.38, larger than for any polyfluorene derivative.[31] Structural studies indicated that these large anisotropy factors are caused by a helical *supramolecular* assembly of the PPE chains rather than by *intra*-chain interactions.

Acknowledgment. We thank Prof. K. Müllen (Max-Planck-Institut für Polymerforschung, MPI-P, Mainz,

Germany) and Prof. H. Möhwald (Max-Planck-Institut für Kolloid- und Grenzflächenforschung, MPI-KG, Golm, Germany) for the opportunity to measure CD spectra in their laboratories. We acknowledge Prof. E. W. Meijer and Dr. Stefan C. J. Meskers (Eindhoven University of Technology, Netherlands) for fruitful discussions of circularly polarized luminescence measurements. We also thank Prof. W. Knoll, Prof. G. Wegner (all MPI-P, Mainz), and Dr. A. Yasuda (Sony International Europe, Stuttgart, Germany) for generous support and fruitful discussions. We further thank Ms. A. Ebert for measuring the absorption spectra in solution. Financial support was given by the Volkswagen Foundation (Germany) and Sony International Europe (Germany). M.O.'s stay was supported in part by a DAAD fellowship.

References and Notes

(1) Bernius, M. T.; Inbasekaran, M.; O'Brien, J.; Wu, W. S. *Adv. Mater.* **2000**, *12*, 1737−1750.
(2) Neher, D. *Macromol. Rapid Commun.* **2001**, *22*, 1366−1385.
(3) Scherf, U.; List, E. J. W. *Adv. Mater.* **2002**, *14*, 477−487.
(4) Grell, M.; Bradley, D. D. C.; Inbasekaran, M.; Woo, E. P. *Adv. Mater.* **1997**, *9*, 798.
(5) Grell, M.; Knoll, W.; Lupo, D.; Meisel, A.; Miteva, T.; Neher, D.; Nothofer, H. G.; Scherf, U.; Yasuda, A. *Adv. Mater.* **1999**, *11*, 671−674.
(6) Lieser, G.; Oda, M.; Miteva, T.; Meisel, A.; Nothofer, H. G.; Scherf, U.; Neher, D. *Macromolecules* **2000**, *33*, 4490−4495.
(7) Sainova, D.; Zen, A.; Nothofer, H.-G.; Asawapirom, U.; Scherf, U.; Hagen, R.; Bieringer, T.; Kostromine, S.; Neher, D. *Adv. Funct. Mater.* **2002**, *12*, 49−57.
(8) Whitehead, K. S.; Grell, M.; Bradley, D. D. C.; Jandke, M.; Strohriegl, P. *Appl. Phys. Lett.* **2000**, *76*, 2946−2948.
(9) Miteva, T.; Meisel, A.; Grell, M.; Nothofer, H. G.; Lupo, D.; Yasuda, A.; Knoll, W.; Kloppenburg, L.; Bunz, U. H. F.; Scherf, U.; Neher, D. *Synth. Met.* **2000**, *111*, 173−176.
(10) Miteva, T.; Meisel, A.; Knoll, W.; Nothofer, H. G.; Scherf, U.; Müller, D. C.; Meerholz, K.; Yasuda, A.; Neher, D. *Adv. Mater.* **2001**, *13*, 565−570.
(11) Oda, M.; Meskers, S. C. J.; Nothofer, H. G.; Scherf, U.; Neher, D. *Synth. Met.* **2000**, *111*, 575−577.
(12) Oda, M.; Nothofer, H. G.; Lieser, G.; Scherf, U.; Meskers, S. C. J.; Neher, D. *Adv. Mater.* **2000**, *12*, 362−365.
(13) Schadt, M. *Annu. Rev. Mater. Sci.* **1997**, *27*, 305.
(14) Peeters, E.; Christiaans, M. P. T.; Janssen, R. A. J.; Schoo, H. F. M.; Dekkers, H. P. J. M.; Meijer, E. W. *J. Am. Chem. Soc.* **1997**, *119*, 9909−9910.
(15) Cisko-Anic, B.; Majeric-Elenkov, M.; Hamersak, Z.; Sunjic, V. *Food Technol. Biotechnol.* **1999**, *37*, 65.
(16) Nothofer, H.-G. *Fluessigkristalline Polyfluorene*; Logos-Verlag: Berlin, 2001.
(17) Rexwinkel, R. B.; Schakel, P.; Meskers, S. C. J.; Dekkers, H. P. J. M. *Appl. Spectrosc.* **1993**, *47*, 731.
(18) Grell, M.; Bradley, D. D. C.; Ungar, G.; Hill, J.; Whitehead, K. S. *Macromolecules* **1999**, *32*, 5810−5817.
(19) Beljonne, D.; Langeveld-Voss, B. M. W.; Shuai, Z.; Janssen, R. A. J.; Meskers, S. C. J.; Meijer, E. W.; Bredas, J. L. *Synth. Met.* **1999**, *102*, 912−913.
(20) Koehler, B.; Enkelmann, V.; Oda, M.; Pieraccini, S.; Spada, G. P.; Scherf, U. *Chem.—Eur. J.* **2001**, *7*, 3000−3004.
(21) Dekkers, H. P. J. M. In *Circular Dichroism*; Berova, N., Nakanishi, K., Woody, R. W., Eds.; Wiley-VCH: New York, 2000.
(22) Berova, N.; Nakanishi, K.; Woody, R. W. *Circular Dichroism*; Wiley-VCH: New York, 2000.
(23) LangeveldVoss, B. M. W.; Janssen, R. A. J.; Christiaans, M. P. T.; Meskers, S. C. J.; Dekkers, H.; Meijer, E. W. *J. Am. Chem. Soc.* **1996**, *118*, 4908−4909.
(24) Lermo, M. E. R.; Langeveld-Voss, B. M. W.; Meijer, E. W. *Abstr. Pap. Am. Chem. Soc.* **1998**, *216*, 577-POLY.
(25) Lermo, E. R.; Langeveld-Voss, B. M. W.; Janssen, R. A. J.; Meijer, E. W. *Chem. Commun.* **1999**, 791−792.
(26) Green, M. M.; Peterson, N. C.; Sato, T.; Teramoto, A.; Cook, R.; Lifson, S. *Science* **1995**, *268*, 1860.
(27) Belletete, M.; Beaupre, S.; Bouchard, J.; Blondin, P.; Leclerc, M.; Durocher, G. *J. Phys. Chem. B* **2000**, *104*, 9118−9125.
(28) Blondin, P.; Bouchard, J.; Beaupre, S.; Belletete, M.; Durocher, G.; Leclerc, M. *Macromolecules* **2000**, *33*, 5874−5879.
(29) Cadby, A. J.; Lane, P. A.; Mellor, H.; Martin, S. J.; Grell, M.; Giebeler, C.; Bradley, D. D. C.; Wohlgenannt, M.; An, C.; Vardeny, Z. V. *Phys. Rev. B* **2000**, *62*, 15604−15609.
(30) Grell, M.; Oda, M.; Whitehead, K. S.; Asimakis, A.; Neher, D.; Bradley, D. D. C. *Adv. Mater.* **2001**, *13*, 577−580.
(31) Wilson, J. N.; Steffen, W.; McKenzie, T. G.; Lieser, G.; Oda, M.; Neher, D.; Bunz, U. H. F. *J. Am. Chem. Soc.* **2002**, *124*, 6830−6831.

MA020630G